

An Experimental Study to Assess the Void Impact on the Ultimate Bearing Capacity of a Strip Footing Sitting on a Reinforced Slope

Omar Zemali

Civil Engineering Laboratory-Risks and Structures in Interactions| Department of Civil Engineering, University of Batna 2, Batna, Algeria
omar.zemali@univ-batna2.dz (corresponding author)

Badis Mazouz

Laboratory of Applied Civil Engineering, Department of Civil Engineering, University of Batna 2, Batna, Algeria
b.mazouz@univ-batna2.dz

Tarek Mansouri

Department of Civil Engineering, University of Batna 2, Batna, Algeria
t.mansouri@univ-batna2.dz

Rafik Boufarh

Department of Civil Engineering, Echahid Cheikh Larbi Tebessi University, Algeria
rafik.boufarh@univ-tebessa.dz

Larbi Djoudi

Department of Civil Engineering, University Mohamed El Bachir El Ibrahimi of Bordj Bou Arreridj, El Anasser, Algeria
Larbi.djoudi@univ-bba.dz

Ahmed Abderraouf Belkadi

Department of Civil Engineering, University Mohamed El Bachir El Ibrahimi of Bordj Bou Arreridj, El Anasser, Algeria
ahmedabderraouf.belkadi@univ-bba.dz

Received: 8 January 2025 | Revised: 27 January 2025 | Accepted: 31 January 2025

Licensed under a CC-BY 4.0 license | Copyright (c) by the authors | DOI: <https://doi.org/10.48084/etasr.10164>

ABSTRACT

This research presents the findings of experimental laboratory models carried out on strip footing situated on a slope with an underlying cavity, considering both unreinforced and geogrid-reinforced soil. Tests were performed on a small-scale footing model subjected to vertical-centric loads. The research encompasses several parametric investigations, varying the cavity depth (H/B), the horizontal distance between the center of the footing and the cavity's center (X/B), and the number of geogrid layers (N). The detailed experimental results indicate that the presence of the cavity diminishes the soil-bearing capacity and undermines slope stability. Furthermore, an increase in cavity depth (H/B), horizontal distance ratios (X/B), and the number of geogrid layers (N) has been shown to result in an enhancement in bearing capacity. Additionally, a variety of failure mechanisms have been observed, with the size of the failure surface and void deformation shape depending on the location of the void and reinforcement layers. In general, the failure area is primarily formed in the direction of the closest void from the foundation and spreads towards the slope.

Keywords-bearing capacity; sand; strip footings; geogrid; void

I. INTRODUCTION

Determining the bearing capacity of structures foundations is a subject in geotechnical engineering that merits particular attention, especially in the context of structures built over subsurface voids. These voids may occur naturally, as evidenced by the presence of underground rivers or limestone dissolution, or they may be artificial, as exemplified by tunnels and quarries. The existence of voids can give rise to significant engineering issues, including foundation instability and the potential for substantial harm to the superstructure. A comprehensive review of the extant literature explores the load-bearing capacity and failure modes of foundations situated on horizontal unreinforced soil with voids. This review employs three main approaches: experimental research, numerical simulations, and theoretical analyses. Authors in [1] applied the upper bound principle of limit analysis to evaluate the impact of strip footing pressure on an underground void and estimate the potential soil collapse above it. The study involved the evaluation of various failure mechanisms related to footing pressure, which led to the development of equations for strip footings positioned over a circular cavity. Authors in [2] employed the upper limit method and 1G loading tests to present and interpret changes in bearing capacity of rigid footings on calcareous sedimentary rock with square cavities. The study identified three failure modes for voids and provided correction equations for the ultimate load-bearing capacity. Authors in [3] employed the Finite Element Method (FEM) program Plaxis to assess the performance of shallow strip footings above twin voids. Their findings indicated that the bearing capacity is influenced by both the size and position of the voids. Authors in [4] created experimental models to assess the impact of voids on the load-bearing capacity of two adjacent footings on granular soil. Their findings indicated that the cavity effect becomes negligible when the distance between the footings and voids exceeds three times the footing width. Additionally, they concluded that a significant cavity depth exists and a critical horizontal distance at which the bearing capacity of the footing diminishes. Authors in [5] examined the seismic bearing capacity of strip footings over square voids. They employed two methods: Adaptive Finite Element Limit Analysis (AFELA) and the pseudo-static approach. The influence of various factors on bearing capacity is provided in design tables and charts. Concurrently, authors in [6] used an AFELA program in conjunction with a pseudo-static approach to assess the seismic bearing capacity of strip footings over cavities in cohesive clay. The study identified three failure mechanisms: roof failure, a mix of roof and wall failure, and bearing failure excluding cavity failure. Authors in [7] examined the influence of a circular cavity on the ultimate bearing capacity of a strip footing under a consistently applied load on rock mass, using adaptive finite element limit analysis. Their numerical simulations validated previous studies, revealing that the void's position influences footing behavior and potential failure envelopes. Furthermore, authors in [8] used lower bound and finite element methods to assess the stability of strip foundations over twin underground cavities. The findings of this study suggest the presence of a rupture zone beneath the foundations, which has the potential to substantially diminish the bearing capacity.

Geogrids have seen a marked increase in utilization for soil reinforcement purposes, owing to their demonstrated efficacy in enhancing load distribution, augmenting shear resistance, and delaying failure. Specifically, the implementation of geogrid layers to strengthen soil above a void has been shown to enhance bearing capacity and mitigate soil settlement. Authors in [9] examined the impact of underground cavities on the bearing capacity and settlement of a strip footing resting on reinforced sand over a void. Their findings indicate that for unreinforced sand, the critical ratio of void depth to diameter is approximately 3.5 to 4. In contrast, for reinforced sand, this ratio varies with relative density and reinforcement. Additionally, the study found that the bearing capacity improves with relative density, the number of geogrid layers, and cavity depth. Authors in [10] conducted laboratory experiments on strip footings with unreinforced and geogrid-reinforced sand with voids to assess footing behavior under repeated loading. Their findings indicated that settlement increases with the presence of a void in the failure area, but decreases with greater void depth and more reinforcement layers. Authors in [11] adopted the Finite Element Analysis (FEA) program PLAXIS 2D to examine the interaction between two neighboring strip footings on unreinforced granular soil with cavity. Their findings suggest that a circular or square void at a depth equivalent to 6 B does not affect the bearing capacity of a single strip footing. Additionally, the absence of a void does not impede the functioning of two interfering strip footings, provided that the spacing ratio exceeds 4B, thereby ensuring each footing operates autonomously. The primary focus of this research was on a strip footing situated on a level surface. Additionally, authors in [12] have examined foundations that rest on reinforced and unreinforced sand slopes devoid of voids. In contrast, there has been a paucity of studies conducted on strip footings near reinforced slopes with voids. Authors in [13] performed experimental analyses to examine the impact of underground circular voids on the bearing capacity of strip footings on the edge of a cohesionless slope under eccentric loads. Their findings revealed that the performance of the strip footing is greatly affected by the cavity and the eccentric loads, especially the void's depth and its horizontal distance from the footing. Authors in [14] conducted numerical analyses to assess the impact of an underground cavity on a shallow strip footing near a reinforced sand slope. The findings of this study indicated the presence of a critical zone beneath the footing where the void does not influence bearing capacity and stability. Furthermore, the incorporation of geogrid reinforcement has been shown to mitigate settlement and enhance bearing capacity. Authors in [15] proposed a laboratory test method to examine the impact of a cavity placed perpendicular beneath a strip footing on a reinforced sand slope. The experiments revealed that using carbon and fiberglass reinforcement significantly increased the bearing capacity by up to 46% relative to glass fibers. The research design entailed conducting laboratory model tests to assess the bearing capacity and failure mechanism of a strip footing on a reinforced sand slope with a circular void aligned parallel to the footing's length, subjected to static vertical loading. To achieve this objective, a total of 140 experimental model tests were conducted, exploring various parameters such

as void depth ratios (H/B), horizontal spacing ratios (X/B), and reinforcement layers (N).

II. EXPERIMENTAL APPARATUS

The experimental model tests were conducted using laboratory trials to evaluate the soil bearing capacity. The model consisted of a steel tank measuring $1.80\text{ m} \times 0.50\text{ m} \times 0.60\text{ m}$ with a fully transparent plexiglass front. The usage of plexiglass in this manner permits the observation of the specimen during preparation and facilitates the discernment of the slope failure mechanism during testing. To prevent potential weakening of the plexiglass due to sand pressure and loads, it was reinforced with two steel columns. The tank's structural integrity is sufficient to resist plane-strain conditions, thereby minimizing out-of-plane displacement. The interior surface of the tank was coated and polished to reduce sand friction, and the load was applied to the footing by sequentially adding weights to the loading system. This method ensures the application of pressure to the soil, which can be adjusted by adding or removing weight. The forces exerted on the footing and soil were measured using an annular dynamometer affixed to the upper structure of the device and connected to the loading system. The dynamometer converts the measured force into a quantifiable value, thereby enabling the user to monitor and record the applied load. The degree of immersion of the footing into the soil was tracked using a displacement sensor, which provided accurate information about the settlement of the soil under load, as shown in Figure 1. This apparatus facilitates the assessment of the behavior and deformation of soils with pure frictional behavior under centered pressure, a critical component in the estimation of their ultimate bearing capacity.



Fig. 1. Experimental apparatus.

III. MATERIALS

A. Geogrid

The geogrid used in the experimental model is the Fortrac Type 80 T shown in Figure 2. It is composed of Polyethylene Terephthalate (PET), with a mesh opening measuring approximately $25\text{ mm} \times 25\text{ mm}$. The maximum longitudinal

tensile strength of the material exceeds or equals 80 kN/m . Table I provides a comprehensive list of the geogrid's various properties.

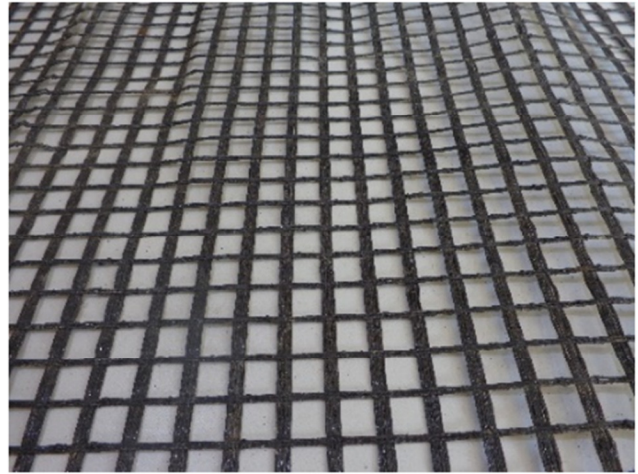


Fig. 2. Geogrid reinforcement used in this study.

TABLE I. GEOGRID PROPERTIES CONSIDERED IN THIS STUDY

Description	Values
Raw Material	PET
Coating	Polymer
Mesh Opening Size	$\approx 25 \times 25\text{ mm}$
Surface Mass	320 g/m^2
Ultimate Longitudinal Tensile Strength	$\geq 80\text{ kN/m}$
Elongation at Nominal Tensile Strength	$\leq 10\%$

B. Soil

The soil used in this study, which was sand, was subjected to analysis in order to ascertain its geotechnical properties in accordance with the standards established by the ASTM. The specific gravity of the sand was determined to be 2.63, and the maximum and minimum dry densities were assessed to calculate the void ratios. The unit weight was determined to be 16.70 kN/m^3 , and the internal friction angle was found to be approximately 38 degrees, suggesting that the sand is dense. According to the Unified Soil Classification System (USCS), the soil is categorized as poorly graded sand (SP). The soil properties are enumerated in Table II.

TABLE II. SOIL PARAMETERS

Properties	Value
Coefficient of uniformity, C_u	3.08
Coefficient of curvature, C_c	1.29
Specific gravity	2.63
Unit weight, γ (kN/m^3) at $D_r = 60\%$	16.70
Maximum dry unit weight (kN/m^3)	19.30
Minimum dry unit weight (kN/m^3)	13.92
Maximum void ratio	0.889
Minimum void ratio	0.362
D_{10} (mm)	0.12
D_{30} (mm)	0.24
D_{60} (mm)	0.37
Effective cohesion, c' (kPa)	0.0
Effective friction angle, ϕ' ($^\circ$)	38.00

C. Cavity

To simulate the presence of a soil cavity, a flexible plastic tube with a diameter of 100 mm and a thickness of 0.6 mm was used. This tube exhibits low resistance, thereby closely simulating a natural cavity devoid of a solid lining. It serves as a representation of the potential alterations that may occur in the soil surrounding the cavity under the influence of loads applied to the soil.

IV. PRESENTATION OF THE CASE STUDY

A total of 140 tests were conducted and meticulously planned to ascertain the inclusion effect of the number of geogrid layers on the bearing capacity of a shallow strip footing placed on a sand slope containing a void. Figure 3 presents the various parameters used to interpret the experimental outcomes, which are expressed as nondimensional factors. These are H/B, X/B, and N, where H/B denotes the vertical distance ratio between the top of the cavity and the bottom of the footing, which was modified within the range of 0.5 to 3.5; X/B signifies the horizontal distance between the center of the footing and the center of the cavity, varying from X/B = 0 to 3; and N indicates the number of layers of the geogrid. The experimental setup involved conducting tests on unreinforced soil and soil reinforced with one, two, and three layers of geogrid. The distance from the base of the footing to the initial geogrid layer, designated as μ , was established at 0.35 B, while the separation between geogrid layers, denoted as h , was set at 0.35B, with B representing the width of the footing. The geogrid length L was systematically maintained at L/B = 4.5 throughout all tests. The values for μ , h , and were selected based on the findings by authors in [9], where it was determined that these values optimize the ultimate bearing capacity. The cavity size was maintained at 1.0 B, and the distance from the slope edge to the footing remained at 0.5 B throughout the study. Table III provides a comprehensive list of the parameters employed in the various parametric tests.

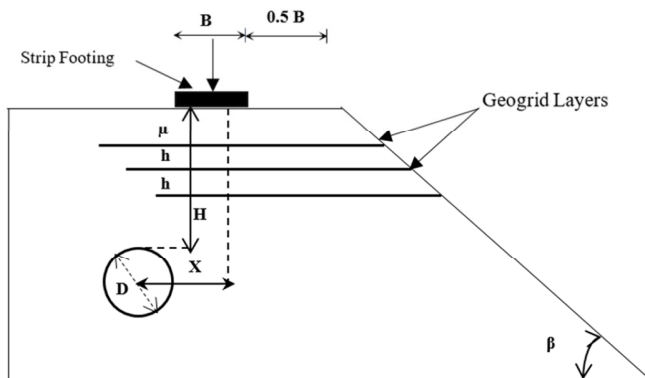


Fig. 3. Geometry parameters.

V. PRESENTATION OF MODEL TEST

The techniques employed to construct the slope are consistent with those described by authors in [16, 17]. Initially, the slope geometry has been delineated on both interior tank walls for reference, shown in Figure 4. The process entails the incremental addition of sand to the tank, with each layer

measuring 5 cm in thickness. The sand is then meticulously compacted using a 60-kg steel roller, ensuring uniform density across the surface. The uniform pressure exerted by the steel roller is ensured by its weight and the smooth surface of the tank.

TABLE III. EXPERIMENTAL PROGRAMS AND PARAMETERS

Test series	Type of reinforcement	Variable parameters			Fixe parameters
		N	X/B	H/B	
1	unreinforced	0	-	No void	$\mu/B=0.35$ $h/B=0.35$ $L/B=4.5$ $\beta=33^\circ$
2	unreinforced with void	0	0.5, 1, 1.5, 2, 2.5, 3	0.5, 1, 1.5, 2, 2.5, 3, 3.5	
3	reinforced	1-2-3	-	No void	
4	reinforced With void	1-2-3	0.5, 1, 1.5, 2, 2.5, 3	5, 1, 1.5, 2, 2.5, 3, 3.5	



Fig. 4. Photographs showing the slope surface preparation for the experiments.

Subsequently, the geogrid reinforcement was positioned on the compacted surface, with a specific fill thickness (u) above the reinforcement layer. During the pouring of the sand, the cavity was simulated by a flexible plastic tube placed in the length of the strip footing. Subsequent to the compaction, the soil surface was excavated and leveled using a metal blade to create a slope with a 33-degree inclination. Subsequent to the application of the load, the weight was transferred from the charge through the footing to the soil, and the pressure force was recorded using a dynamometer. Concurrently, the displacement sensor monitored any positional changes in the footing to measure soil displacement.

VI. RESULTS AND DISCUSSION

A strip footing bearing capacity over a cavity on a sandy slope with a 33-degree incline was tested 140 times, with the footing distance from the slope crest maintained constant ($b/B = 0.5$). The following discussion will present the laboratory test results and discuss the effects of various parameters, as outlined in Table III. The void positions were adjusted both vertically (H/B) and horizontally (X/B) from the footing. As presented in Figure 5, the bearing capacity values were determined using the tangent intersection method, as outlined by authors in [18].

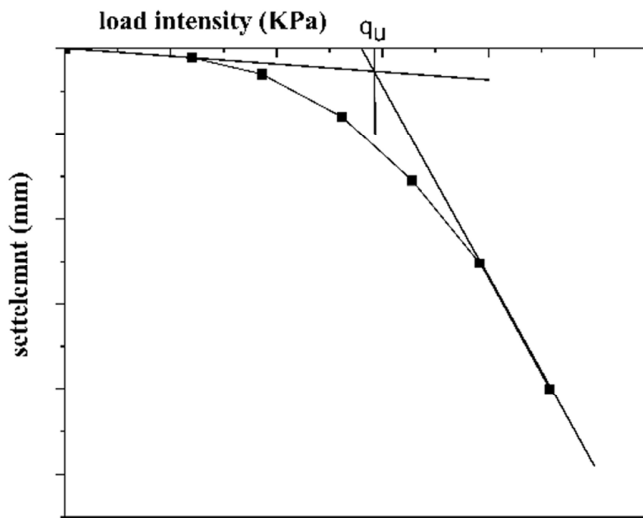


Fig. 5. The Tangent Intersection Method is used to interpret the ultimate bearing capacity (q_u).

The findings were examined using two reduction factors to quantify the effects of voids and geogrid layers on bearing capacity. The initial reduction factor, designated as BCR_u , signifies the ratio of the load-bearing capacity of the footing on unreinforced sand with and without voids, respectively, as:

$$BCR_u = \frac{q_{uv}(\text{with a void})}{q_u(\text{with no void})} \tag{1}$$

The second reduction factor is the bearing capacity ratio (BCR_r). In this equation, q_{uvr} is the bearing capacity of a strip footing on a reinforced slope with a cavity, and q_u is the bearing capacity of the same strip footing on an unreinforced slope without a cavity:

$$BCR_r = \frac{q_{uvr}(\text{with a void})}{q_u(\text{with no void})} \tag{2}$$

A. Effect of location of the void

As shown in Figure 6, the variation of the reduction factor (BCR_u) with respect to different embedment depths (H/B) from 0.50 to 3.5 for varying horizontal distance ratios (X/B), ranging from 0.5 to 3, is demonstrated. Figure 6 indicates that cavity depth exerts a substantial influence on the soil bearing capacity ratio, particularly when the void distance ratios H/B and X/B are 0.5 and 0, respectively. The proximity of the footing to the void, in conjunction with the thin sand layers beneath the

footing, resulted in observed instability between the soil and adjacent voids. It has been demonstrated that increasing the H/B ratio leads to a reduction in pressure on the upper portion of the void crest, consequently decreasing the footing settlement and enhancing the bearing capacity.

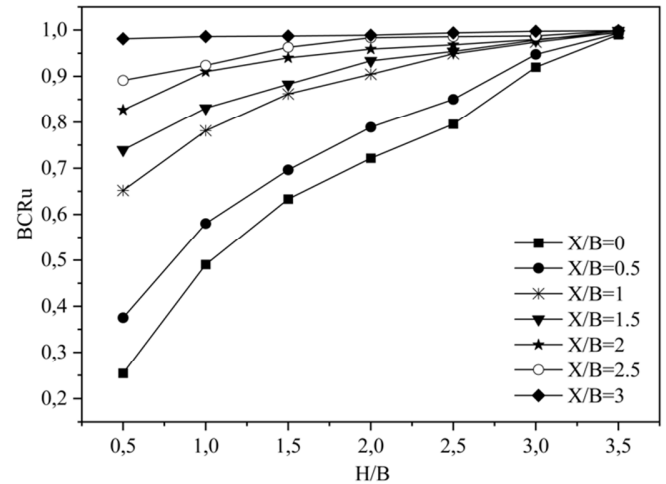


Fig. 6. Variation in ultimate bearing capacity BCR_u , as a function of H/B with different horizontal spacing X/B .

The soil bearing capacity ratio increases with cavity depth for all X/B values, reaching a maximum at $H/B = 3.5$, which is known as the critical depth ($H_{cr} = 3.5$). Beyond this critical depth, the influence of the void vanishes, akin to soil devoid of a cavity [19]. Conversely, as X/B increases, BCR_u increases irrespective of the impediment depth void H/B until reaching a critical horizontal value of $X/B = 3$ ($X_{cr} = 3 B$). A higher X/B ratio has been shown to decrease void deformation and minimize the cavity's impact on the footing's stress field, leading to greater BCR_u values. When $X/B = 3$, the BCR_u approaches 1 and remains constant, rendering the void effect negligible across all H/B magnitudes.

B. Effect of Geogrid Layers

The implementation of geogrid layers has been demonstrated to enhance soil shear resistance and restrict lateral movements. This enhances soil rigidity and mitigates settling, particularly in regions with voids. As presented in Figure 7 (a), the variation bearing capacity ratio (BCR_r) is contingent upon the number of geogrid layers (N), the horizontal distance ratio (X/B), and the vertical distance ratios (H/B). As shown in Figure 7, the bearing capacity ratio (BCR_r) is significantly influenced by the number of geogrid layers and the position of the cavity in relation to the footing. It is evident from the figure that when $H/B=1.5$, BCR_r exhibits a consistent increase with the number of geogrid layers (N) for all values of X/B ratios. This observation signifies that the incorporation of geogrid reinforcement enhances the load-bearing capacity of strip footing while concurrently reducing the effect of the cavity. This enhancement can be attributed to the geogrid's ability to distribute stresses within the soil mass, thereby augmenting its overall shear strength and stiffness, particularly on slopes where voids generate zones of weakness.

Additionally, the augmentation of soil cover atop the void and reinforcement layer, in conjunction with arching motions, has been demonstrated to enhance soil-bearing capacity and mitigate settlement. The introduction of a solitary geogrid layer has been demonstrated to enhance the soil-bearing capacity ratio by up to 122%. The integration of two layers has been shown to augment this capacity to 149%, while the implementation of three layers has been observed to elevate the ratio to 164%. As shown in Figure 7 (b), the presence of a void at a depth of 3.5 B does not affect the load-bearing capacity of a strip footing for three layers of reinforcement ($N = 3$). At $H/B = 3.5$ ($H_{cr}=3.5$), the bearing capacity ratio value remains constant for each geogrid layer, irrespective of the horizontal distance X/B . This finding suggests that the soil's bearing capacity is comparable to that of reinforced sand devoid of voids. This observation is consistent with the observed convergence of the BCR_r values around three layers. Conversely, at $H_{cr}=3.5$, the cavity's influence becomes negligible, resulting in closer BCR values across all X/B ratios. This outcome indicates that the influence of the number of geogrid layers becomes predominant beyond a critical position (H_{cr} and X_{cr}). Conversely, minimal BCR values are observed at low X/B and H/B ratios (e.g., $X/B = 0$), necessitating supplementary reinforcement to ensure stability.

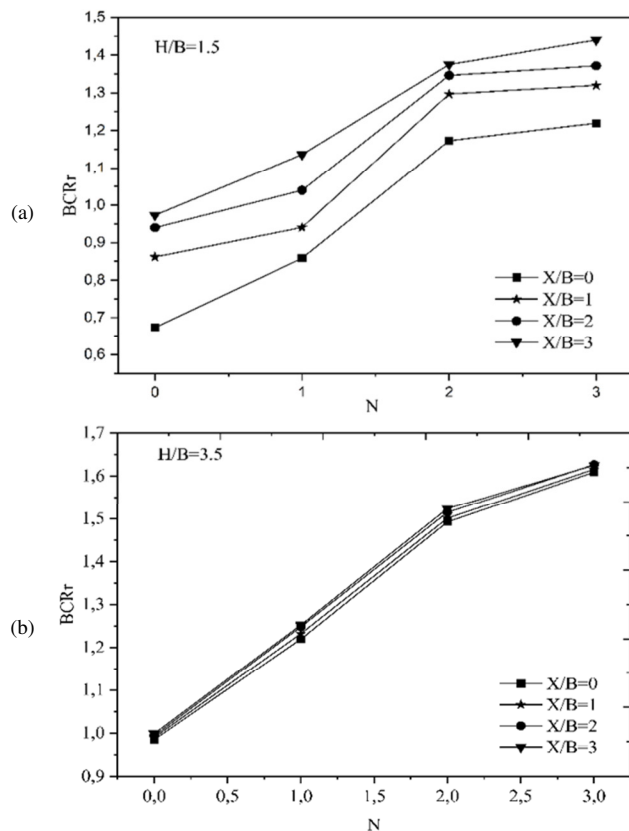


Fig. 7. Variation in ultimate bearing capacity BCR_r as a function of N with different horizontal spacing X/B : (a) $H/B=1.5$, (b) $H/B=3.5$.

VII. FAILURE MECHANISM

The interaction of a shallow strip footing with a geogrid-reinforced sand slope and underlying void gives rise to complex failure mechanisms. Figures 8, 9, and 10 show the failure mechanisms and the void's deformation for a strip footing placed on both reinforced and unreinforced sand slopes under centric loading. As presented in these figures, the evolution of failure mechanisms is found to be substantially influenced by the void's position and the number of geogrid layers. Furthermore, it has been observed that deformation in the void decreases with increasing embedment depth ratios H/B , the horizontal distance ratio X/B , and geogrid layers N . It is also noteworthy that if H/B or X/B exceeds 3.5 and 3, respectively, no deformation is observed, indicating that the void is located outside the rupture zone. In such scenarios, the failure mechanism resembles that of a strip footing on sand with no void, as shown in Figures 8 (c) and 9 (c).

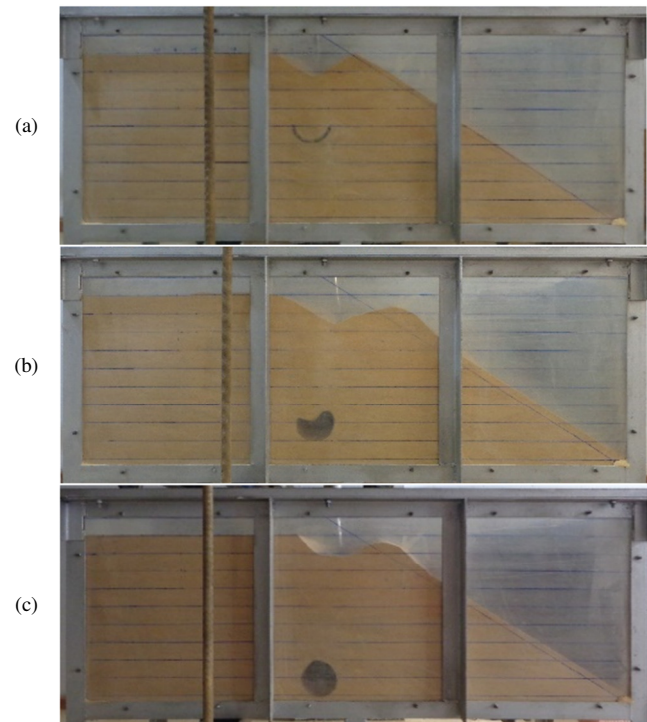


Fig. 8. Failure mechanisms of reinforced sand slope : (a) $H/B = 1.5$, (b) $H/B = 3.0$, (c) $H/B = 3.5$ and $X/B = 0$.

However, the presence of a cavity within the rupture zone results in alterations to the effective stress distribution, thereby creating a weak zone at the slope's face and around the void's edges. This, in turn, leads to a substantial reduction in the soil's bearing capacity and overall stability. The failure mechanism initiates on the footing side, extends toward the void, and propagates toward the slope. In the case of an unreinforced sand, with X/B and H/B lower than a critical distance ($H_{cr} = 3.5$ and $X_{cr} = 3$), an unstable triangular zone is created underneath the foundation, leading to failures under varying loading conditions. The geometry of this zone undergoes alterations in conditions conducive to reinforced sand.

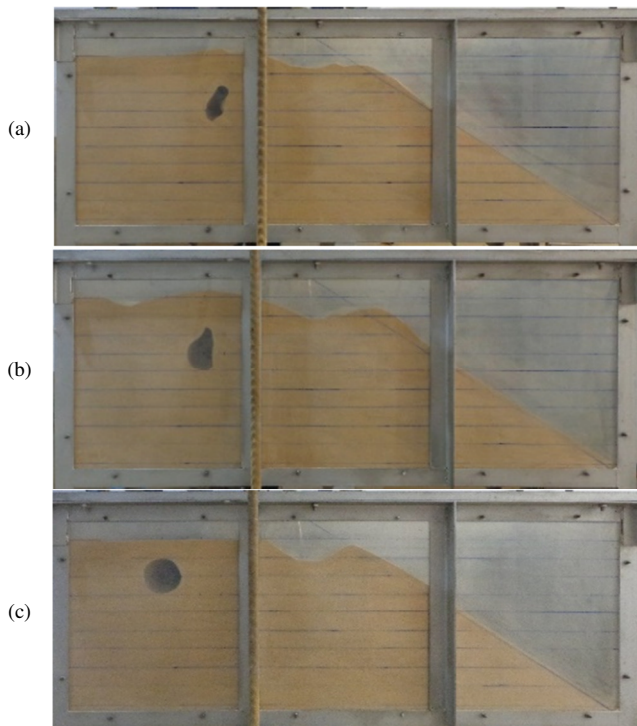


Fig. 9. Failure mechanisms of reinforced sand slope: (a) $X/B = 1.5$, (b) $X/B = 2$, (c) $X/B = 3$ and $H/B = 0.5$.

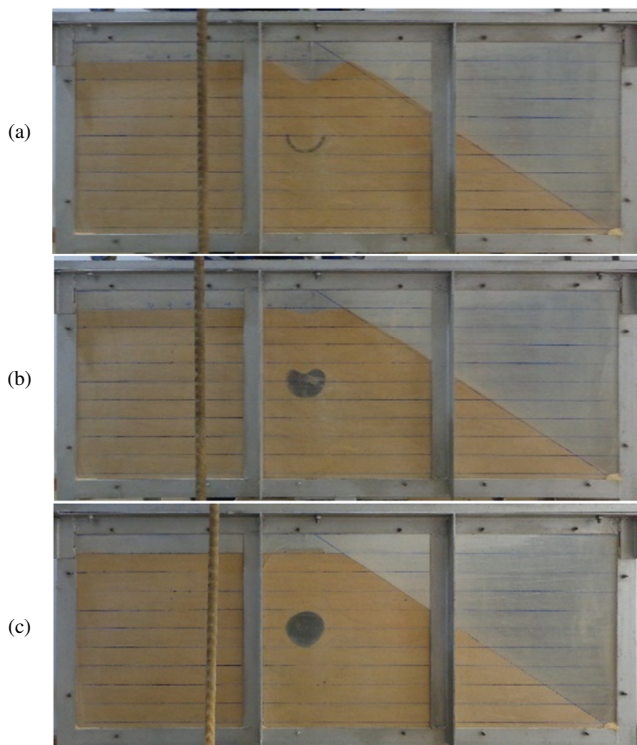


Fig. 10. Failure mechanisms of reinforced sand slope : (a) $N = 0$, (b) $N = 1$, (c) $N = 2$ with $X/B = 0$ and $H/B = 1.5$.

However, the presence of geogrid reinforcement, in conjunction with the friction between the sand and geogrid,

impeded the descent of the triangular wedge, thereby causing a transformation into a trapezoidal zone. It is evident that the incorporation of reinforcement significantly enhanced the ultimate load capacity of the footing and the displacement required to attain failure. The study further observed that the number of reinforcing layers played a pivotal role in averting void failure, mitigating void deformation, and impeding the footing and soil from penetrating below into the void. The presence of three reinforcement layers ensured the stability of the void, and it is hypothesized that the adverse effects of the void on the footing's behavior will be completely mitigated, as presented in Figure 10.

VIII. CONCLUSIONS

This experimental study analyzed the impact of void on the bearing capacity and failure mechanisms of strip footing placed near reinforced sand slopes with various geometries. The ensuing observations are derived from the experimental model tests:

- The study found that voids invariably reduce the load-bearing capacity of strip footing, both in the absence of reinforcement and in the presence of reinforcement.
- The impact of a single void on bearing capacity becomes negligible when the void is located at a critical depth exceeding $3.5 B$ and at a horizontal distance more than $3 B$ from the footing's center.
- The insertion of geogrid reinforcement has been observed to enhance bearing capacity and diminish settlement of the strip footing.
- Increasing the number of reinforcing layers significantly augments bearing pressure and mitigates settlement.
- The presence of various failure surfaces has been identified, with the dimensions and void deformation shape contingent on the location of the void and the reinforcement layers.

REFERENCES

- [1] M. C. Wang and C. W. Hsieh, "Collapse Load of Strip Footing Above Circular Void," *Journal of Geotechnical Engineering*, vol. 113, no. 5, pp. 511–515, May 1987, [https://doi.org/10.1061/\(ASCE\)0733-9410\(1987\)113:5\(511\)](https://doi.org/10.1061/(ASCE)0733-9410(1987)113:5(511)).
- [2] M. Kiyosumi, O. Kusakabe, and M. Ohuchi, "Model Tests and Analyses of Bearing Capacity of Strip Footing on Stiff Ground with Voids," *Journal of Geotechnical and Geoenvironmental Engineering*, vol. 137, no. 4, pp. 363–375, Apr. 2011, [https://doi.org/10.1061/\(ASCE\)GT.1943-5606.0000440](https://doi.org/10.1061/(ASCE)GT.1943-5606.0000440).
- [3] A. A. Lavasan, A. Talsaz, M. Ghazavi, and T. Schanz, "Behavior of Shallow Strip Footing on Twin Voids," *Geotechnical and Geological Engineering*, vol. 34, no. 6, pp. 1791–1805, Dec. 2016, <https://doi.org/10.1007/s10706-016-9989-6>.
- [4] D. Saadi, K. Abbeche, and R. Boufarh, "Model experiments to assess effect of cavities on bearing capacity of two interfering superficial foundations resting on granular soil," *Studia Geotechnica et Mechanica*, vol. 42, no. 3, pp. 222–231, Jun. 2020, <https://doi.org/10.2478/sgem-2019-0046>.
- [5] Y. Xiao, M. Zhao, and R. Zhang, "Seismic bearing capacity for strip footings above voids in cohesive-frictional soils," *Earthquake Spectra*, vol. 39, no. 1, pp. 269–287, Feb. 2023, <https://doi.org/10.1177/87552930221141110>.
- [6] R. Zhang, M. Feng, Y. Xiao, and G. Liang, "Seismic Bearing Capacity for Strip Footings on Undrained Clay with Voids," *Journal of*

- Earthquake Engineering*, vol. 26, no. 9, pp. 4910–4923, Jul. 2022, <https://doi.org/10.1080/13632469.2020.1851316>.
- [7] V. B. Chauhan, P. Kumar, and S. Keawsawasvong, "Limit Analysis Solution for Ultimate Bearing Capacity of Footing Resting on the Rock Mass with a Circular Void Subjected to Line Loading," *Indian Geotechnical Journal*, vol. 53, no. 2, pp. 334–347, Apr. 2023, <https://doi.org/10.1007/s40098-022-00676-2>.
- [8] J. M. Rouchi and M. A. Nozari, "Effect of Twin Circular Underground Voids on Bearing Capacity of Strip Foundations," *European Journal of Engineering Science and Technology*, vol. 6, no. 2, pp. 1–13, 2023, <https://doi.org/10.33422/ejest.v6i2.1137>.
- [9] S. N. Moghaddas Tafreshi, O. Khalaj, and M. Halvae, "Experimental study of a shallow strip footing on geogrid-reinforced sand bed above a void," *Geosynthetics International*, vol. 18, no. 4, pp. 178–195, Aug. 2011, <https://doi.org/10.1680/gein.2011.18.4.178>.
- [10] A. Asakereh, S. N. Moghaddas Tafreshi, and M. Ghazavi, "Strip footing behavior on reinforced sand with void subjected to repeated loading," *International Journal of Civil Engineering*, vol. 10, no. 2, pp. 139–152, Jun. 2012.
- [11] A. Benbouza, T. Mansouri, and K. Abbeche, "Behavior of Strip Footing/s above Void in Sandy Soil," *Engineering, Technology & Applied Science Research*, vol. 13, no. 1, pp. 10039–10044, Feb. 2023, <https://doi.org/10.48084/etasr.5494>.
- [12] B. Mazouz, K. Abbeche, A. Abdi, and M. Baazouzi, "Model experiments to assess effect of eccentric loading on the ultimate bearing capacity of a strip footing near a dry sand slope," *International Journal of Geotechnical Engineering*, vol. 15, no. 10, pp. 1241–1251, Nov. 2021, <https://doi.org/10.1080/19386362.2019.1665385>.
- [13] T. Mansouri, R. Boufarh, and D. Saadi, "Effects of underground circular void on strip footing laid on the edge of a cohesionless slope under eccentric loads," *Soils and Rocks*, vol. 44, May 2021, Art. no. e2021055920, <https://doi.org/10.28927/SR.2021.055920>.
- [14] B. Mazouz, T. Mansouri, M. Baazouzi, and K. Abbeche, "Assessing the Effect of Underground Void on Strip Footing Sitting on a Reinforced Sand Slope with Numerical Modeling," *Engineering, Technology & Applied Science Research*, vol. 12, no. 4, pp. 9005–9011, Aug. 2022, <https://doi.org/10.48084/etasr.5131>.
- [15] B. Azeddine and M. Abdelghani, "The cavity's effect on the bearing capacity of a shallow footing in reinforced slope sand," *Soils and Rocks*, vol. 46, Jan. 2023, Art. no. e2023003622, <https://doi.org/10.28927/SR.2023.003622>.
- [16] C. Yoo, "Laboratory investigation of bearing capacity behavior of strip footing on geogrid-reinforced sand slope," *Geotextiles and Geomembranes*, vol. 19, no. 5, pp. 279–298, Jul. 2001, [https://doi.org/10.1016/S0266-1144\(01\)00009-7](https://doi.org/10.1016/S0266-1144(01)00009-7).
- [17] E. Sawwaf and M. A. "Strip Footing Behavior on Pile and Sheet Pile-Stabilized Sand Slope," *Journal of Geotechnical and Geoenvironmental Engineering*, vol. 131, no. 6, pp. 705–715, Jun. 2005, [https://doi.org/10.1061/\(ASCE\)1090-0241\(2005\)131:6\(705\)](https://doi.org/10.1061/(ASCE)1090-0241(2005)131:6(705)).
- [18] K. Ueno, K. Miura, and Y. Maeda, "Prediction of Ultimate Bearing Capacity of Surface Footings with Regard to Size Effects," *Soils and Foundations*, vol. 38, no. 3, pp. 165–178, Sep. 1998, https://doi.org/10.3208/sandf.38.3_165.
- [19] A. Badie and M. C. Wang, "Stability of Spread Footing Above Void in Clay," *Journal of Geotechnical Engineering*, vol. 110, no. 11, pp. 1591–1605, Nov. 1984, [https://doi.org/10.1061/\(ASCE\)0733-9410\(1984\)110:11\(1591\)](https://doi.org/10.1061/(ASCE)0733-9410(1984)110:11(1591)).